Serb. Astron. J. № 171 (2005), 19 - 27
DOI: 10.2298/SAJ0571019C

UDC 524.3 – 82
Original scientific paper

EFFECTS OF LOCALIZED HORIZONTAL FLOW PATTERNS ON EIGENFREQUENCIES OF STELLAR GLOBAL MODES

V. M. Čadež[1] and P. Vanlommel[2]

[1]*Astronomical Observatory, Volgina 7, 11160 Belgrade 74, Serbia and Montenegro*

[2]*Royal Observatory of Belgium, Ringlaan 3, B-1180 Brussels, Belgium*

(Received: November 4, 2005; Accepted: November 11, 2005)

SUMMARY: The main goal of this paper is to estimate the significance of effects the flow profile $U_0(z)$ induces on computed global oscillation spectra. We solve numerically the eigenvalue problem for the described basic state configuration with reference to solar conditions as an example of a typical star. Obtained results show that the considered shear flows do not only affect the eigenfrequencies ω but they also have an impact on spatial profiles of eigensolutions of linearized physical quantities. Such flows may even allow for local amplification of perturbation amplitudes at positions where the resonant Doppler condition $\omega = kU_0(z)$ is satisfied. For typical subsonic flow speeds this Doppler resonant wave amplification can be effective only in the case of the non acoustic gravity modes with sufficiently large horizontal wavenumbers k.

Key words. Sun: helioseismology – Stars: oscillations

1. INTRODUCTION

It is well known that a star can exhibit various types of bulk oscillations that are equivalent to helioseismic modes observed on the Sun and seismic modes of the Earth. If magnetic field effects are excluded, these global oscillations are known to be in three characteristic groups of eigenmodes: a set of pressure driven acoustic p-modes, a single incompressible surface f-mode and a set of gravity driven g-modes. The p-modes are being observed on the Sun and some of their frequencies can be precisely determined with relative errors reaching 10^{-5}.

All these modes are spatially localized and have perturbation amplitude distributions with one or more peaks located in the stellar interior. A thorough overview on helioseismology and its application in stellar diagnostics can be found in Gough and Toomre (1991), Christensen-Dalsgaard et al. (1998) and Christensen-Dalsgaard (1998).

Spectral properties of global oscillations depend on physical parameters describing the chosen stellar model. This includes geometrical structuring of the interior and atmosphere of a star, the related temperature and density profiles, chemical composition and kinematic state of the ambient plasma, and possible magnetic field distribution. Among important stellar features affecting global modes are also macroscopic motions of convective and meridional flows often encountered at stellar surface regions. In the case of the Sun, effects of such motions on global eigenspectra have been extensively treated so far. For example, Murawski and Roberts (1993a,b), Murawski and Goossens (1993) studied the f mode by solving an extended dispersion relation which involves random horizontal flows in a plane-parallel model of the upper layers of the Sun while Pranab et al. (1995) considered other velocity profiles. Stein and Nordlund (1998) numerically simulated the granulation near the solar surface, while Rosenthal et al. (1999) applied hydrodynamical simulations in two computational models: the reduced-gamma model and the gas-gamma model using the mixing-length theory.

In this work, our attention is focused on patterns of spatially localized horizontal flows and their influence on stellar global seismic modes. In particular, we are interested in achieving a better insight into sensitivity of modal eigenfrequencies on flow profiles alone. The model we consider assumes a gravitationally stratified gaseous structure composed of three distinct layers with prescribed temperature distributions, simulating three typical stellar regions: the interior, overlaying convection layer with a localized nonuniform flow U_0 beneath the stellar surface, and a static atmosphere-corona above it. Physical quantities of the basic state are taken z-dependent in the Cartesian geometry, with the z-axis oriented along the gravity vector. This paper is thus an extension of our previous studies of global modes (Vanlommel and Čadež 1998 2000, Vanlommel and Goossens 1999) related to purely static configurations.

We take now the macroscopic flow velocity to be horizontal with the speed $U_0(z)$ varying and changing its sign in the vertical direction z which resembles motion patterns of elongated horizontal convective cells in the Cartesian geometry. The analytical expression for the model velocity profile $U_0(z)$ is chosen as to allow a convection zone to be simulated by a pile of elongated convective cells with conserved total mass fluxes. The flows are taken in opposite directions at the horizontal cell edges but retain the same orientation through the boundary between adjacent cells. Free parameters specifying such a flow pattern are taken to be the speed c normalized to some typical value at the surface $z = 0$, the number n of layers of piled convective cells within the convection layer and the parameter p determining the distribution of the flow speed inside the convective cell.

For a basic state prescribed by a chosen reference set of related physical parameters, we solved the eigenvalue problem numerically by utilizing boundary conditions requiring the energy density of linear perturbations to vanish at large $|z|$, and the vertical displacement $\xi_z(z)$ caused by fluid motions and the pressure perturbation $P(z)$ to be continuous at boundaries separating the layers. The resulting modal eigenfrequencies ω and eigensolutions $\xi_z(z)$ and $P(z)$ show the dispersion curves and localization domains of different global modes with horizontal wavelength $\lambda = 2\pi/k$ taken along the direction of the flow. The obtained dispersion diagram (k, ω) shows discrete parabolic lines in domains bounded by cut-off curves. The numerical procedure was performed for ranges of flow parameters which yields the eigenfrequency dependence on flow characteristics. This approach of relating eigenfrequency variations to changes in the basic state parameters is an alternative to the methods of inverse techniques (for example Gough and Toomre 1983, Basu et al. 2000 and references therein) based on the variational principle and knowledge of kernels which are functions of the reference basic state and eigensolutions. Our numerical method of solving the eigenvalue problem for a sequence of basic states can be applied to any $z-$dependent basic state configuration prescribed initially.

As to the applicability of the Cartesian geometry in our analysis, it is valid only for perturbations of a sufficiently small wavelength λ ($R_* \gg \lambda$) when the effects of stellar sphericity are unimportant.

The paper is organized as follows: the unperturbed equilibrium model is described in Section 2, the basic equations for linear perturbations and the eigenvalue solutions are found in Section 3, the numerical results with plots showing frequency shifts of global modes when the flow parameters are varied, can be seen in Section 4 while Section 5 contains a discussion of results and conclusions.

2. MODEL OF UNPERTURBED STATE

Following the approach of our previous paper (Vanlommel and Čadež 2000, hereafter VC2000), we consider a basic stellar model composed of three nonuniform regions in the Cartesian geometry: an isothermal atmosphere ($z \le 0$), a convection zone of thickness W ($W \ge z > 0$) with a constant adiabatic temperature gradient, and a convectively stable stellar interior ($z \ge W$) with a constant and sub-adiabatic temperature gradient. Stratification of the medium is thus along the uniform gravity $\vec{g} = g\hat{e}_z$ in the $z-$direction. Nonuniform horizontal fluid motions $\vec{v}_0 = U_0(z)\hat{e}_x$ are assumed to exist in the convection layer while the fluid is at rest elsewhere.

The stellar plasma is taken as an ideal and fully ionized gas composed of protons and electrons, initially in a stationary equilibrium:

$$\nabla p_0 + \rho_0(\vec{v}_0 \cdot \nabla)\vec{v}_0 = \rho_0 \vec{g} \tag{1}$$

with the $z-$axis oriented toward the stellar interior.

As $\rho_0(\vec{v}_0 \cdot \nabla)\vec{v}_0 = 0$ for horizontal $z-$dependent motions, the flow patterns we consider do not affect the initial hydrostatic balance in which case Eq. (1) reduces to the expression for a static equilibrium as used in VC2000. The following basic state temperature and density profiles are therefore assumed:

$$T_0(z) = T_c \begin{cases} \tau, & z < 0 \\ 1 + \Gamma \dfrac{z}{H}, & 0 \le z \le W \\ c_i + \mathcal{A}\Gamma \dfrac{z - W}{H}, & z \ge W \end{cases} \tag{2}$$

with

$$c_i \equiv 1 + \Gamma \frac{W}{H} \quad \text{and} \quad \Gamma \equiv (\gamma - 1)/\gamma.$$

as shown schematically in Fig. 1. Here, $\mathcal{A}$ is a dimensionless parameter determining the sub-adiabatic temperature gradient in the stellar interior ranging between $\mathcal{A} = 0$ (the isothermal temperature profile) and $\mathcal{A} = 1$ (the adiabatic temperature profile);

$\tau \equiv T_a/T_c$ where $T_a = T_c\tau$ and T_c are temperatures of the stellar atmosphere (the corona) and the top of the convection zone respectively; $T_i = c_i T_c$ is the temperature at the transition from the convection zone to the stellar interior (at $z = W$). The remaining quantities have their standard meanings.

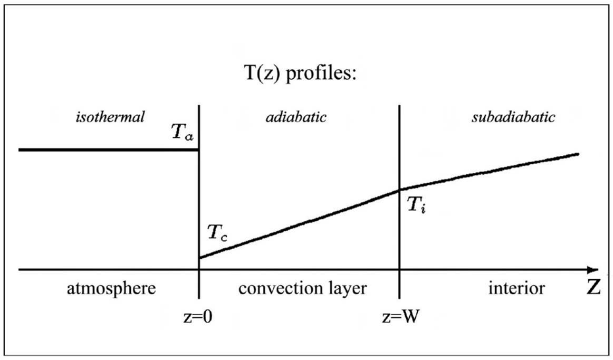

Fig. 1. *Schematic temperature profile in the atmosphere (the corona), convection zone and stellar interior.*

The density distribution $\rho_0(z)$ follows from Eqs. (1)-(2) as:

$$\rho_0 = \rho_c \begin{cases} \left(c_i{}^{m_c} + \mathcal{A}\Gamma \dfrac{z-W}{H}\right)^{m_i}, & z \geq W \\ \left(1 + \Gamma \dfrac{z}{H}\right)^{m_c}, & 0 \leq z \leq W \\ \frac{1}{\tau}\, \mathrm{e}^{z/\tau H}, & z < 0 \end{cases} \tag{3}$$

where ρ_c is a reference density at $z = 0$ while m_c and m_i, known as polytropic indices, are given by:

$$m_c \equiv \frac{1}{\gamma - 1} \quad \text{and} \quad m_i \equiv \frac{1}{\mathcal{A}\Gamma} - 1.$$

In our one-dimensional approach, all macroscopic motions are taken to be horizontal like in the case of elongated convective cells whose side edges (with vertical motions) are far apart from each other in comparison with the wavelength of perturbations and to the thickness W of the convection layer. Flows $U_0(z)$ are taken to cause no net mass flux Φ_m through the normal cross-sectional plane of any individual cell:

$$\Phi_m \equiv \int_0^{W/n} \rho_0(z) U_0(z) dz = 0. \tag{4}$$

The integer parameter $n = 1, 2, ...$ denotes the number of stacked convective cells within the convection layer of thickness W.

A suitable model function describing such a flow pattern can be taken in the following form:

$$U_0(z) = \frac{cU_0\rho_c}{\rho_0(z)} \left[\cos \frac{n\pi z}{W}\right]^{2p+1}. \tag{5}$$

The parameters $p = 1, 2, ...$ and $c = 0, 1, 2, ...$ (Fig. 2) determine respectively: the flow concentration at horizontal cell boundaries, and scaling of some reference flow speed U_0 at $z = 0$.

In a special example that follows, we shall take the stellar basic state parameters relevant to solar conditions.

3. EIGENVALUE PROBLEM FOR LINEAR PERTURBATIONS

The described basic state is subject to isentropic linear harmonic perturbations having frequency ω and the horizontal wavenumber k which can also be expressed in terms of the degree l by $k^2 = l(l+1)/R_*^2$ ($R_*^2 \equiv R_\odot = 696$ Mm - the Solar radius). To remain within the applicability of the Cartesian geometry, the wavelength $\lambda \equiv 2\pi/k$ must be sufficiently small as to satisfy the condition $R_\odot \gg \lambda$ which is equivalent to $l \gg 2\pi \approx 6$. In this case, the degree l and the horizontal wavenumber k are mutually related as $l \approx kR_\odot$. These perturbations are governed by standard equations of fluid dynamics which reduce to two linear equations for the vertical displacement ξ_z and the perturbed pressure P:

$$\begin{aligned} D\frac{\mathrm{d}\xi_z}{\mathrm{d}z} &= C_1\xi_z - C_2 P, \\ D\frac{\mathrm{d}P}{\mathrm{d}z} &= C_3\xi_z - C_1 P. \end{aligned} \tag{6}$$

The coefficients D, C_1, C_2 and C_3 are given by

$$\begin{aligned} &D(z) = \rho_0(z) v_s^2(z) \Omega^2(z), \\ &C_1(z) = -\rho_0(z) g \Omega^2(z), \\ &C_2(z) = \Omega^2(z) - \omega_s^2(z), \\ &C_3(z) = \rho_0^2(z)\Omega^2(z) v_s^2(z) \left[\Omega^2(z) - \omega_{\mathrm{BV}}^2(z)\right]. \end{aligned} \tag{7}$$

where Ω, ω_s and ω_{BV} are the Doppler shifted wave frequency ω, the sound frequency and the Brunt-Väisälä frequency respectively, defined as:

$$\begin{aligned} &\Omega \equiv \omega - kU_0(z), \quad \omega_s^2 \equiv v_s^2 k^2 \quad \text{and} \\ &\omega_{\mathrm{BV}}^2(z) \equiv g\left[(\gamma - 1)\frac{g}{v_s^2(z)} - \frac{\mathrm{d}}{\mathrm{d}z} \ln T_0(z)\right]. \end{aligned} \tag{8}$$

The medium is locally stable regarding the convective instability if $\omega_{\mathrm{BV}}^2(z) > 0$. In the basic state we consider, this is true in the solar corona and interior while the unstable convection zone tends to establish approximately the adiabatic temperature gradient yielding $\omega_{\mathrm{BV}}^2(z) = 0$.

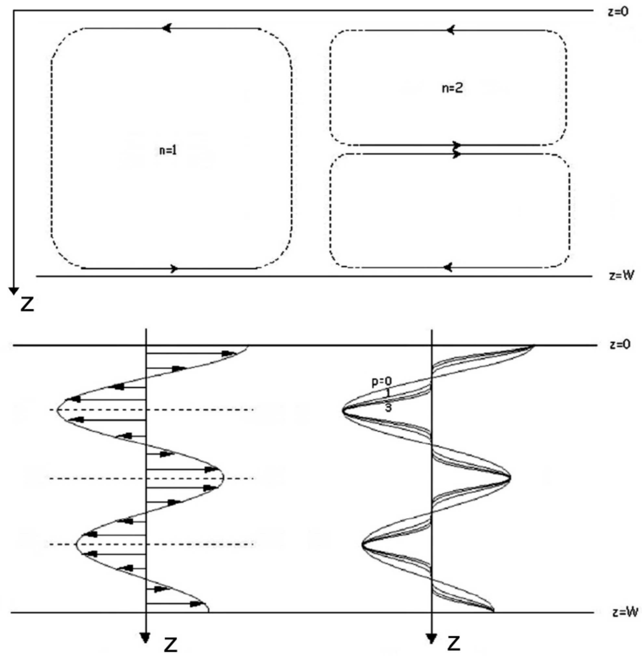

Fig. 2. *Schematic representation of flow profiles $U_0(z)$ for different n, c and p: The upper figures illustrate a single cell and a stack of two cells, $n = 1$ and $n = 2$, respectively. The lower figures show variation of the normalized flow speed with z (left) and the distribution of the flow concentration within a cell determined by the parameter p (right) for $n = 4$.*

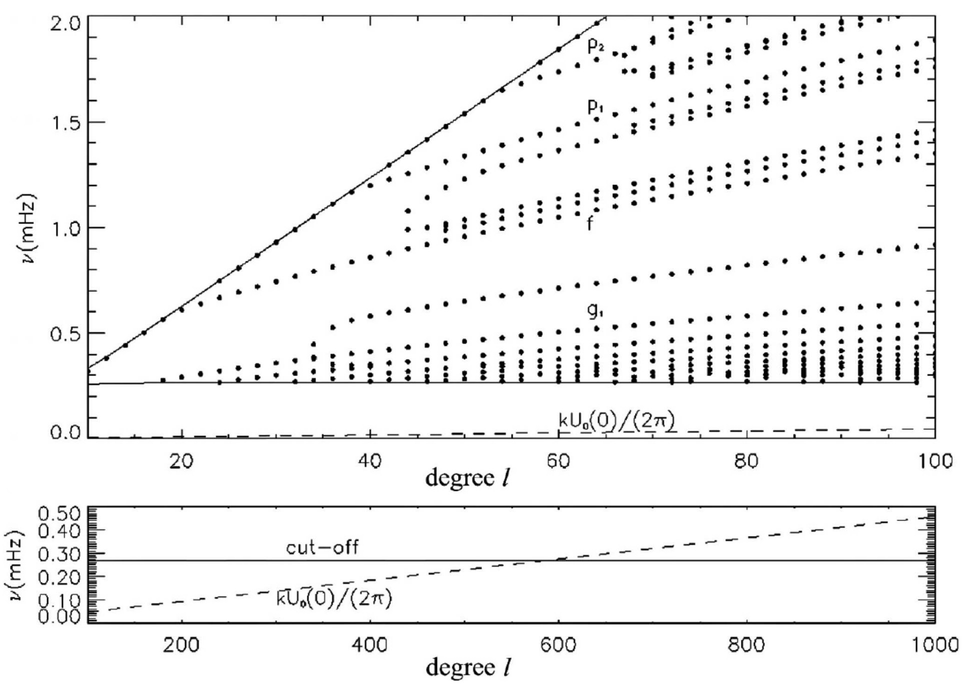

Fig. 3. *Obtained dispersion curves for $c = 1$, $n = 1$ and $p = 0$ showing splitting of basic acoustic modes arising from the layered structure of the unperturbed model. The slanted and horizontal solid lines are the upper and lower cut-off frequency curves related to the atmosphere and interior respectively. The dashed line below the lower cut-off is the resonant line $\nu = lU_0(0)/(2\pi R_*)$ ($k \approx l/R_*$ for $l \gg 6$). An expanded view of the cut-off and the resonant line is shown in the lower plot.*

Eqs. (6) are solved analytically in the coronal region and in the solar interior, and numerically in the convection zone. The obtained solutions are matched through the boundary conditions that require continuity of ξ_z and P at $z = 0$ and $z = W$. As global modes are spatially localized, the solutions of Eq. (6) have also to satisfy the boundary condition at infinity requiring the energy density of perturbations to vanish at $|z/H| \gg 1$ (far in the corona and deep in the interior). The resulting analytical solutions are exponentially decreasing functions of z in the isothermal corona ($z < 0$) and a combination of two confluent hypergeometric functions $\mathcal{U}(z)$ and $\mathcal{M}(z)$ (Abramowitz and Stegun 1965) in the subadiabatic solar interior ($z > W$).

The eigenvalue problem now reduces to finding pairs of eigenvalues (ω, k) for which the global eigensolutions satisfy the required boundary conditions at $z = W$ and $z = 0$. The full description of the corresponding numerical scheme can be found in our earlier paper (Vanlommel and Čadež 1998) in which static basic states were studied. Now, the presence of a flow introduces some new features to eigensolutions: in addition to shifts in eigenfrequencies, a nonuniform flow may cause a local resonant instability at $z = z_r$ where $\Omega(z_r) = 0$. At this location, Eqs. (6) have a second order Doppler-type singularity in which a phase matching or resonant interaction between the global mode and the flow takes place: $\omega = kU_0(z_r)$. Consequently, an instability develops when the amplitude of the mode grows in time by gaining energy from the flow. As the linear amplitudes grow, the neglected nonlinearities and plasma dissipations become important and cannot be ignored anymore, which eventually leads to a saturation of growth. The linear approach therefore only points out the fact that a resonance exists where the linear solutions diverge. A full analysis of eigensolutions in the vicinity of a resonance requires a nonlinear approach and taking dissipations into account. In our case, the divergent linear solutions can easily be obtained in an asymptotic form in the domain $z \approx z_r$ where Eqs. (6) reduce to a single equation:

$$\frac{\mathrm{d}}{\mathrm{d}z}\left[(z - z_r)^2 \frac{\mathrm{d}\xi_z}{\mathrm{d}z}\right] + \frac{\omega_{\mathrm{BV}}^2(z_r)}{(U_0')^2}\xi_z = 0, \qquad (9)$$

with $U_0' \equiv \mathrm{d}U_0(z)/\mathrm{d}z|_{z=z_r} \neq 0$ and $\omega_{\mathrm{BV}}^2(z_r) \geq 0$ in the considered basic state,. Eq. (9) has two types of solutions depending on the sign of $|U_0'| - 2\omega_{\mathrm{BV}}(z_r)$:

If $|U_0'| \geq 2\omega_{\mathrm{BV}}(z_r)$, the solution is

$$\xi_z = a_1|z - z_r|^{(\mu - 1/2)} + \frac{a_2}{|z - z_r|^{(\mu + 1/2)}} \qquad (10)$$

with

$$\mu = \frac{\left[(U_0')^2 - 4\omega_{\mathrm{BV}}^2(z_r)\right]^{1/2}}{2|U_0'|}.$$

If $|U_0'| \leq 2\omega_{\mathrm{BV}}(z_r)$, the solution is

$$\begin{aligned}\xi_z &= a_1\frac{\cos(\mu_1 \ln|z - z_r|)}{|z - z_r|^{1/2}} + \\ &+ a_2\frac{\sin(\mu_1 \ln|z - z_r|)}{|z - z_r|^{1/2}} \qquad (11)\end{aligned}$$

where a_1 and a_2 are integration constants and $\mu_1 \equiv |\mu|$. In either case, the solution to the linear vertical displacement ξ_z diverges at $z = z_r$ if dissipations and nonlinearities are ignored.

4. NUMERICAL RESULTS

To make the effects of the flow more noticeable and comparable with results of a static case, we choose the same typical values for the basic state parameters as in VC2000: $T_c = 4170K$ for the temperature at the top of the convection zone, the temperature ratio at $z = 0$ is $\tau = 400$ and the subadiabatic temperature gradient is determined by $\mathcal{A} = 0.8$ and the depth of the convection zone is $W = 0.3\,R_\odot$. This basic state is now extended by a macroscopic plasma flow in the convection zone whose speed profile is given by Eq. (5) with $U_0 = 2000$ m/s and variable parameters n, p and c. A numerical solution of the eigenvalue problem for linear perturbations in such a basic state yields dispersion curves $\omega = \omega(l)$ for global modes: the acoustic p-mode, the gravity g-mode, and the surface f-mode, shown in Fig. 3. As seen, the diagram of dispersion curves is rather complex as additional branches of dispersion curves appear due to the fact that the considered basic state is composed of individual layers separated by sharp boundaries which eventually introduces new modes.

The inclusion of macroscopic flows into the convection zone results into frequency shifts of the whole pattern of dispersion curves. Details of how these shifts depend on the flow parameters c, p and n are shown in Figs. 4-6 respectively for eigenfrequencies related to the degree $l = 100$. The influence of the flow is comparable for both the acoustic and gravity modes.

According to Fig. 4, the shift of the reference frequency (related to $l = 100$) grows almost linearly with the flow intensity parameter c for the $f-$ and p_1-mode if c increases from 0 to 1. This tendency holds also for acoustic modes of higher order. We can also notice that the related growth rates increase with the modal order i: the frequency of the p_i-mode is shifted more than the frequency of the $p_{i-1}-$mode; the same is true also for the g_i-modes. A variation of the flow profile parameter p causes the reference frequency to decrease with p for the $f-$ and p_1-modes, as seen in Fig. 5. The shapes of curves $\Delta\nu = \Delta\nu(p)$ showing the negative frequency shifts for p_i- and g_i-modes, depend on the modal order i in a more complex way. Analogous features are also observed in Fig. 6 if the number of piled cells n is varied. The frequency shifts are negative and of several times larger magnitude than those caused by varying p within the chosen interval.

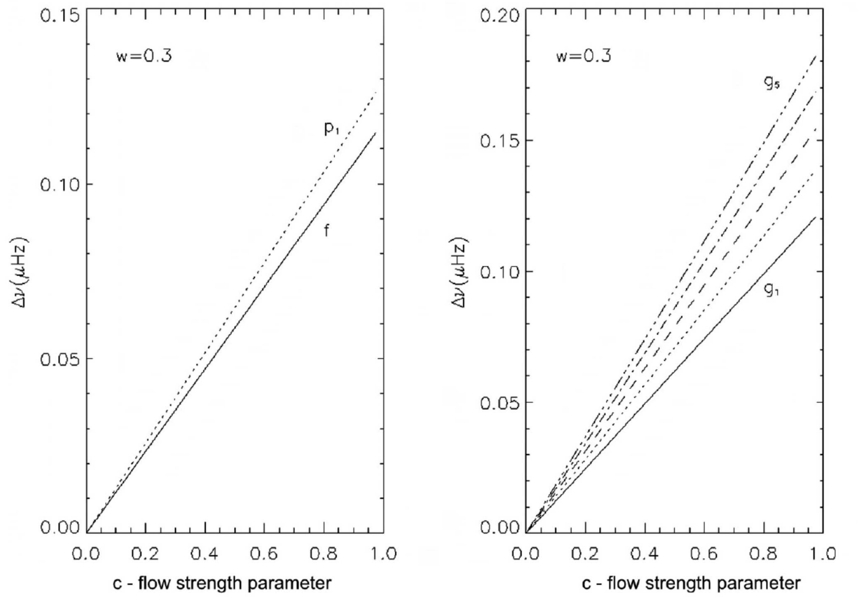

Fig. 4. *Frequency shifts $\Delta\nu = \nu(c) - \nu(c = 0)$ at different values of the flow parameter c. Other quantities are fixed: $n = 1$, $p = 0$ and $l = 100$.*

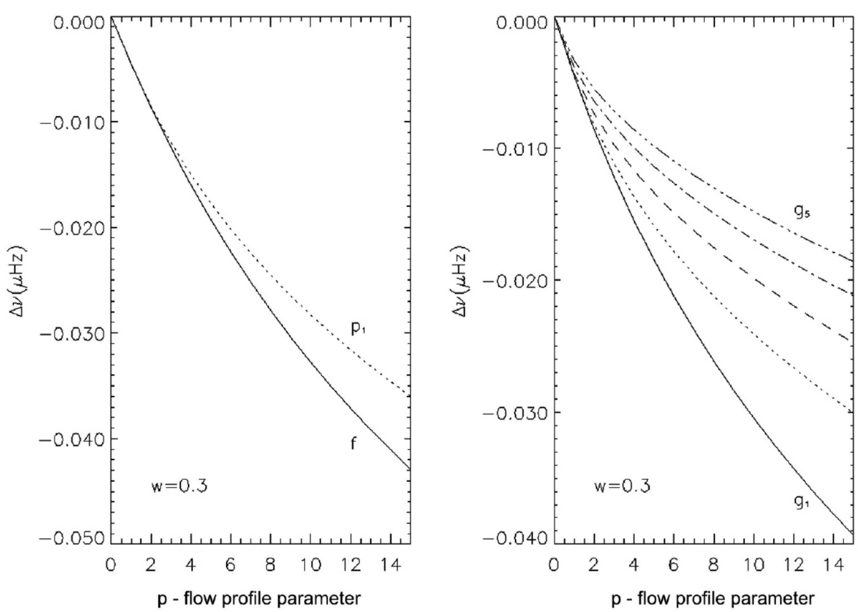

Fig. 5. *Frequency shifts $\Delta\nu = \nu(p) - \nu(p = 0)$ at different values of the flow parameter p. Other parameters are fixed: $c = 1$, $n = 1$ and $l = 100$.*

Fig. 7 shows the solution for the perturbed pressure in the convection zone ($0 \leq z/H \leq 2145$) as a function of z/H for the f, p_1 and the first three $g-$modes. The eigensolutions are not plotted in the corona nor in the interior where their amplitudes are negligible in comparison with those in the convection zone where the modes are predominantly present.

As already said, the nonuniform horizontal flows also allow for a Doppler type singularity where the flow is in resonance with global modes. For typical solar conditions, this can occur at sufficiently large degrees l where the flow term $kU_0(z)$ exceeds the lower cut-off frequency for $g-$modes. As $|U_0(z)| \leq |U_0(0)|$ in the considered model flow profile, we plot (the lower graph in Fig. 3) the resonant line $\nu \equiv \omega/2\pi \approx lU_0(0)/(2\pi R_\odot)$ as a boundary separating the domain with allowed resonances (frequencies below the resonant line) from the domain in which the resonance cannot occur (frequencies above the resonant line). Consequently, the low frequency gravity waves can resonate with the flow if their frequency ν exceeds the lower cut-off and satisfies the condition $\nu \leq U_0(0)/(2\pi R_\odot)$ at the same time. This can take place only after the resonant line crosses the lower cut-off at sufficiently large degree l as seen in the lower plot in Fig. 3. As to the acoustic modes, their frequencies are too high and they cannot get into resonance with subsonic flows - their dispersion curves do not intersect the $kU_0(0)$-line.

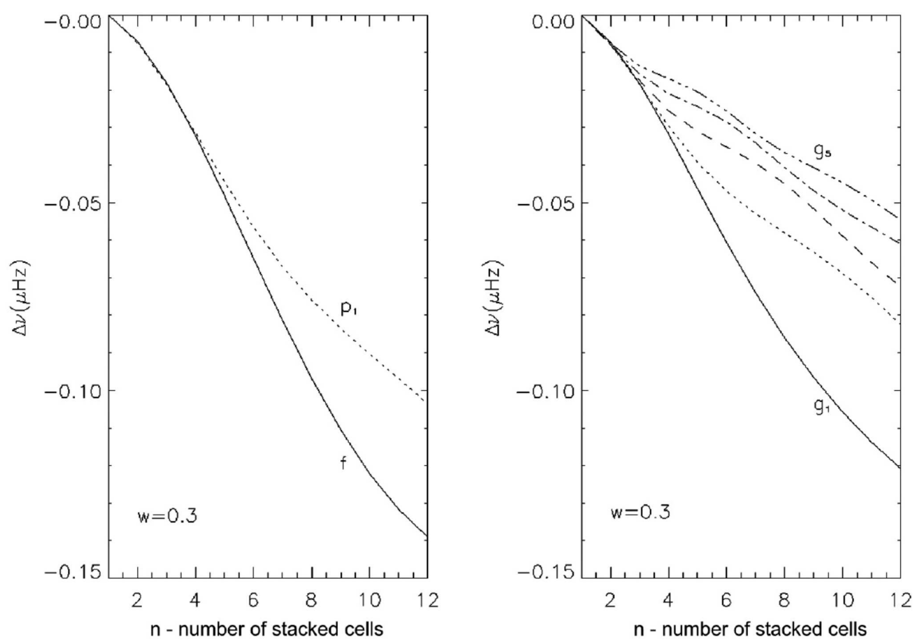

Fig. 6. *Frequency shift $\Delta\nu = \nu(n) - \nu(n=0)$ at different values of the flow parameter n. Other parameters are fixed: $c = 1$, $p = 0$ and $l = 100$.*

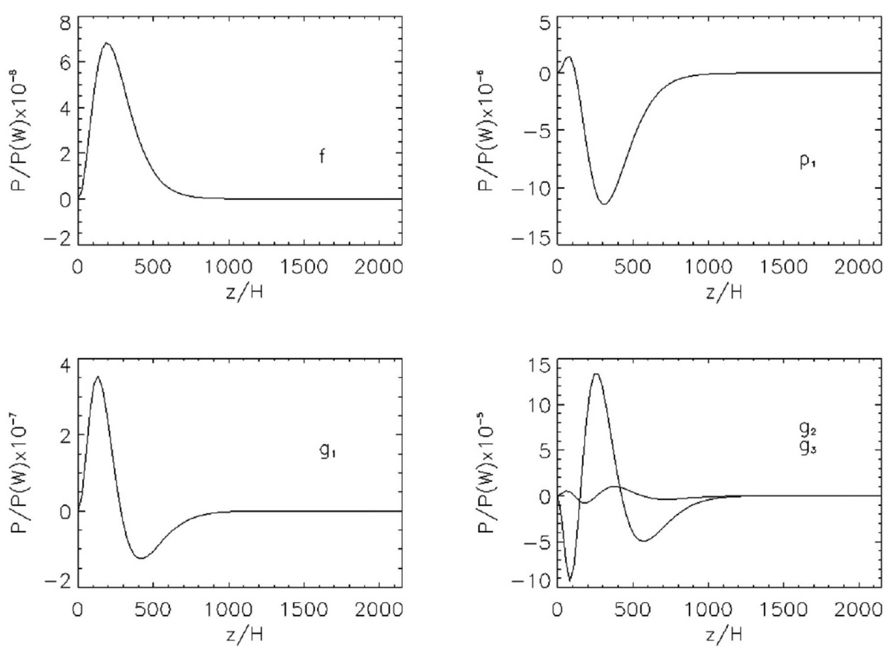

Fig. 7. *Eigensolutions for the dimensionless pressure perturbation $P(z/H)$ for the f, p_1 and the first three $g-$modes with $l = 100$. The flow parameters are $c = 1$, $n = 1$ and $p = 0$.*

5. CONCLUSI0NS

The main object of this study is to estimate the effects of large scale horizontal motions on stellar global modes for models discussed in our earlier papers (Vanlommel and Čadež 1998, 2000, Vanlommel and Goossens 1999).

The eigenfrequency spectra are computed from boundary conditions applied to localized solutions of linearized fluid dynamics equations at boundaries $z = 0$ and $z = W$ separating the atmosphere (the corona) from the convection zone and the convection zone from the interior respectively. In the considered numerical example of the basic state, we chose physical parameters relevant to the Sun.

The obtained eigensolutions for the vertical displacement ξ_z and pressure perturbation P are localized mostly below the surface $z = 0$ while the precise locations of their extrema depend on characteristics of the flow profile.

The computed eigenspectra experience a typical Sturmian behaviour for the p_i modes and an anti Sturmian for the g_i modes. We point out that if the Cartesian geometry is fully applicable ($l \gg 6$) as in our case, the existence of modes with different order i is not a consequence of the spherical geometry, they arise from the linear temperature profile in the region below the convection zone, and from properties of solutions given in terms of confluent hypergeometric functions.

Magnitudes of frequency shifts are of the order of 10^{-2} to 10^{-1} μHz as presented in Figs. 4-6. The parameter c that scales the speed of the flow, has the most pronounced effect on eigenfrequency variations as also found by Gough and Toomre (1983) by applying a variational method. Changes in c cause larger frequency shifts than variations of the remaining two parameters p and n related to the profile of the flow and to the number of piled convective cells respectively.

If the flow parameters are $c = 1$, $p = 0$ and $n = 1$, the relative frequency shift is $1.5 \cdot 10^{-4}$ for the g_1 mode with $l = 100$, and $5 \cdot 10^{-5}$ for the p_1 mode. This shift is of the order of the observational accuracy for the solar p modes that reaches 10^{-5}.

Another consequence of nonuniform flows in the convection zone is a possibility for a Doppler resonance occurring when the condition $\Omega(\omega_r, l) = 0$ is satisfied. The limiting resonant curve $\nu = lU_0(0)/(2\pi R_\odot)$ is plotted in Fig. 3. In our model, the resonance can happen only for high degree g modes with $l > 600$ when these modes can resonantly be amplified by nonuniform horizontal flows in the convection zone. Consequently, such a resonant wave amplification of $g-$modes arising from nonuniform subphotospheric flows may lessen the difficulties of their observational detection at the solar surface.

Acknowledgements – V. M. Čadež acknowledges the support by the ESA PRODEX (Ulysses) and the Belgian Federal Services for Scientific, Technical and Cultural Affairs during his stay at the Belgian Institute for Space Aeronomy. This work has been completed at the Belgrade Astronomical Observatory within the project "Solar spectral irradiance variation" (No. 1951) supported by the Ministry of Sience and Environmental Protection of the Republic of Serbia.

REFERENCES

Abramowitz, M. and Stegun, I. A.: 1965, Handbook of Mathematical Functions, Dover Publications, Inc., New York.

Basu, S., Pinsonneault, M. H. and Bahcall, J. N.: 2000, *Astrophys. J.*, **529**, 1084.

Bell, A.R.: 1978a, *Mon. Not. R. Astron. Soc.*, **182**, 147.

Christensen-Dalsgaard, J., Däppen, W., Dziembowski, W.A. and Guzik, J.A.: 1998, Variable Stars as Essential Astrophysical Tools. Proc. NATO Advanced Study Institute, ed. C. Ibanogher, Kluwer Acad. Publ., 59.

Christensen-Dalsgaard, J.: 1998, Lecture Notes on Stellar Oscillations, Fourth Edition, Institute of Physics and Astronomy, University of Arhus, Arhus, Denmark. `http://www.obs.aau.dk/~jcd/oscilnotes/`

Gough, D. O. and Toomre, J.: 1983, *Solar Phys.*, **82**, 401.

Gough, D. O. and Toomre, J.: 1991, *Annu. Rev. Astron. Astrophys.*, **29**, 627.

Murawski, K. and Goossens, M.: 1993, *Astron. Astrophys.*, **279**, 225.

Murawski, K. and Roberts, B.: 1993a, *Astron. Astrophys.*, **272**, 595.

Murawski, K. and Roberts, B.: 1993b, *Astron. Astrophys.*, **272**, 601.

Pranab Ghosh, Antia, H.M. and Chitre, S.M.: 1995, *Astrophys. J.*, **451**, 851.

Rosenthal, C.S., Christensen-Dalsgaard, J., Nordlund Å, Stein, R.F. and Trampedach, R.: 1999, *Astron. Astrophys.*, **351**, 689.

Stein, R.F. and Nordlund, Å: 1998, *Astrophys. J.*, **499**, 914.

Vanlommel, P. and Čadež, V. M.: 1998, *Solar Phys.*, **182**, 263.

Vanlommel, P. and Goossens, M.: 1999, *Solar Phys.*, **187**, 357.

Vanlommel, P. and Čadež, V. M.: 2000, *Solar Phys.*, **196**,227.

УТИЦАЈИ ПРОФИЛА ЛОКАЛИЗОВАНИХ ХОРИЗОНТАЛНИХ ПРОТИЦАЊА НА СОПСТВЕНЕ ФРЕКВЕНЦИЈЕ ЗВЕЗДАНИХ ГЛОБАЛНИХ МОДОВА

V. M. Čadež[1] and P. Vanlommel[2]

[1]*Astronomical Observatory, Volgina 7, 11160 Belgrade 74, Serbia and Montenegro*

[2]*Royal Observatory of Belgium, Ringlaan 3, B-1180 Brussels, Belgium*

UDK 524.3 – 82
Оригинални научни рад

Разматра се утицај локализованих хоризонталних суб-фотосферских протицања различитих профила на фреквенције сеизмичких глобалних модова звезда и Сунца. Модел претпоставља равну геометрију са $z-$осом усмереном дуж вектора гравитације ка унутрашњости звезде. Средина је идеалан гас и има вишеслојну структуру која симулира типичне области звезде: њену унутрашњост, конвективну зону са протицањем и атмосферу – корону. Свака од тих области има свој линеарни профил температуре, густине и притиска и налази се у стању хидростатичке равнотеже.

За такво основно стање решен је сопствени проблем за линеарне пертурбације које су хармонијске у времену и у хоризонталном правцу док им амплитуде зависе од промењљиве z. Аналитичка решења у виду хипер-геометријских функција као и нумеричка решења за област постојања протицања датог профила, задовољавају граничне услове под условом да је задовољена дисперзиона једначина која повезује фреквенцију и хоризонтални таласни број и која се одређује нумеричком методом. Показано је постојање Доплеровске резонанце која доводи до линеарне нестабилности и амплификације амплитуда пертурбација. У случају Сунца, таква резонанца би могла да повећа амплитуде одређених таласа гравитационих модова захваљујући чему би могли лакше да се детектују.